Meteorology and Atmospheric Physics (2019) 131:697–712
https://doi.org/10.1007/s00703-018-0597-2

ORIGINAL PAPER

Precursory strong-signal characteristics of the convective clouds of the Central Tibetan Plateau detected by radar echoes with respect to the evolutionary processes of an eastward-moving heavy rainstorm belt in the Yangtze River Basin

Yang Zhao[1,2] · Xiangde Xu[2] · Zheng Ruan[2] · Bin Chen[2] · Fang Wang[2]

Received: 12 July 2017 / Accepted: 28 February 2018 / Published online: 15 March 2018

Abstract
The integrated analysis of the data from a C-band frequency-modulated continuous-wave (C-FMCW) radar site in Naqu obtained during a rainstorm over the middle and lower reaches of the Yangtze River and the data concerning the three-dimensional structure of the circulation of the precipitation system that occurred over the lower reaches of the Yangtze River Basin during the Third Tibetan Plateau (TP) Atmospheric Experiment from August 15th to 19th, 2014, was carried out. The changes in the echo intensity at the C-FMCW radar site in Naqu were of regional indicative significance for the characteristics of the whole-layer apparent heat source Q1 in local areas and the region of the adjacent river source area, including the Yangtze River, Yellow River, and Lancang River (hereinafter referred to as the "source area of three rivers"), as well as to the vertical speeds due to the development of convection. This study indicates that the C-FMCW radar echo intensity of the plateau convection zone and the related power structures of the coupled dipole circulations in the middle layer of the atmosphere, as well as in the upper atmospheric level divergence and lower atmospheric level convergence, are important stimuli for convective clouds in this region. Furthermore, these radar data provided a physical image of the development and maintenance mechanisms of an eastward-moving heavy rainstorm belt. This study also shows that changes in the echo intensities at the C-FMCW radar site of Naqu can provide strong signals related to heavy rainstorm processes in the upper reaches of the Yangtze River.

1 Introduction

Located in the central region of the Asian continent, the Tibetan Plateau (TP) contains complex landforms and has the highest elevation of any plateau in the world. In the summer, the TP is the site of a huge thermodynamic pump, which is of vital importance to the hydrological cycle of East Asia and the rest of the world. China is susceptible to various extreme weather events (e.g., rainstorms), and it suffers frequent disastrous weather events. The frequency of these extreme rainstorm events in summer and their difficulty to predict can lead to extensive flooding and landslides in the Chinese mainland. The previous studies have shown that the convective precipitation systems and cloud structures over the TP can indicate the genesis of extreme rainstorm events over the Yangtze River Basin, including those over its lower reaches (Yanai et al. 1992; Xu and Chen 2006).

For many years, the occurrence and development mechanisms of extreme rainfall in the middle and lower reaches of the Yangtze River Basin and the weather systems of the TP have been topics on the forefront of academic research in the field of meteorology. The topographic effects of the TP on both regional and global atmospheric water circulations, as well as summer monsoons in Asia, have also been heavily discussed issues in the international research community (Boos and Kuang 2010). In the late 20th century, many scholars attempted to study the influences of the precipitation systems of the TP on the genesis and development of extreme weather events and the climate of the Yangtze

Responsible Editor: S.-W. Kim.

✉ Xiangde Xu
xuxd@cma.gov.cn

[1] Nanjing University of Information Science and Technology, Jiangsu 210044, China

[2] State Key Laboratory of Severe Weather, Chinese Academy of Meteorological Sciences, Beijing 100081, China

River Basin. However, research related to this issue is beset with various difficulties resulting from the sparse distribution of observational stations over the TP. To ascertain the weather and climate effects of the TP, the China Meteorological Administration and Chinese Academy of Science have jointly carried out several atmospheric observational and experimental campaigns in the TP. Using data from the First TP Atmospheric Experiment, Qin (1983) analyzed the characteristics of the convective clouds at the observation station in Naqu, Tibet. During the Second TP Atmospheric Experiment, researchers analyzed the characteristics of diurnal precipitation variations during convection processes using Doppler radar (Liu et al. 1999, 2015). Zhuo et al. (2002) observed the following phenomena with respect to an extraordinary rainstorm process that occurred over the Yangtze River Basin in 1998: (1) cloud clusters over the TP moved distinctly eastward as time progressed; (2) the main movement tracks of the convective cloud clusters showed a trend of movement away from the TP to areas that experienced extraordinary rainstorm events over the middle and lower reaches of the Yangtze River; and (3) cloud clusters were further developed during this eastward movement. The vertical structures characterized by upper level airflow divergence and lower level airflow convergence constituted a prerequisite for the eastward movement of the convective cloud clusters in the atmosphere over the TP. Chang and Guo (2016) analyzed the data from the Third TP Atmospheric Experiment, which were obtained in 2014 (e.g., heights of cloud bases and tops, diurnal precipitation variations, and precipitation characteristics), and they demonstrated the diversity of the convective clouds and diurnal precipitation variations in Naqu. Due to the lack of observational convective cloud data from the TP, most researchers performed statistical analyses of the convective precipitation and cloud structures in the atmosphere over the TP using unconventional data, such as satellite observations (Fu et al. 2007; Cai et al. 2012). Using data from the World Wide Cloud (WWC), Hu et al. (2016) analyzed the characteristics of the tracks of convective clouds in the atmosphere over the TP. Using satellite observation data, Fujinami and Yasunari (2001) concluded that the convective clouds of the TP in the summer are enhanced after 12:00 (local time) and peak at 18:00 (local time).

Liu et al. (2015) noted that the C-band frequency-modulated radar for continuous vertical observations represented China's first cloud and precipitation observation system and that it has a frequency-modulated continuous-wave (FMCW) aggregate state and phase mode. Using data concerning the echo intensities of the Doppler radar and radial velocity observations in Naqu, Uyeda et al. (2001) uncovered the basic characteristics of the convective clouds in the atmosphere over the TP during the main period of the summer monsoon. Using radar observation data collected over 3 months, Zhuang and Liu (2012) developed a new scanning algorithm to reduce the influences of landforms on the echoes and applied this algorithm to the observations of convective clouds in Naqu. Likewise, Bringi et al. (2001) developed a new algorithm to improve the observations of convective rainfall using the echoes of C-band FMCW (C-FMCW) radar and applied this algorithm to the South China Sea monsoon experiment. Using C-FMCW radar, Jin et al. (2016) described the characteristics of cloud structures in the atmosphere of the TP. During the Third TP Atmospheric Experiment, convective rainfall events were observed using the echoes of a C-FMCW radar site in Naqu in the central TP region (as shown in Fig. 1).

The rainfall over the TP mostly comprises convective rainfall. Flohn (1968) estimated the density of cumulonimbi in the TP via a satellite cloud image. This study found that the huge cumulonimbi in the southeastern region of the TP caused a chimney effect on the heat transport in the upper atmosphere, indicating that the topographic effect of the TP contributes to the generation of strong convective clouds. Recently, atmospheric science researchers have expressed heightened concern over whether the convective clouds in the atmosphere over the TP possess strong-signal characteristics with respect to the early stages of rainstorm events over the middle and lower reaches of the Yangtze River. The corresponding research projects employing radar applications for sky observations have mainly focused on the characteristics of local convective clouds or on the observational capabilities of radar. The correlations between the radar echoes and atmospheric circulation characteristics over the lower reaches of the TP still require further study.

The purpose of this paper is to uncover the links between the genesis, development, and spatiotemporal evolutions of rainstorms over eastern China with activity over the lower reaches of the TP and to investigate the strong-signal characteristics of the convection systems in the atmosphere over the TP detected by C-FMCW radar echoes. Based on the dynamic changes in the echoes of the C-FMCW radar observed during August 2014, this paper probes the predictive strong-signal characteristics of convective clouds (observed via radar echoes in Naqu) over the central TP with respect to the genesis and development of an eastward-moving rainstorm belt over the middle and lower reaches of the Yangtze River. To verify the applicability of the results of this research, this paper also presents the correlation between the total cloud cover of Naqu in the summer and that over all of China in the summers from 1961 to 2010. As shown in Fig. 1, the total cloud cover of Naqu in August is significantly correlated with the cloud systems over the regions ranging to its lower reaches. Specifically, the observational stations that yield data with credibility values of 90% or higher revealed an east–west rain belt with high correlations to cloud cover. The calculation results indicate that

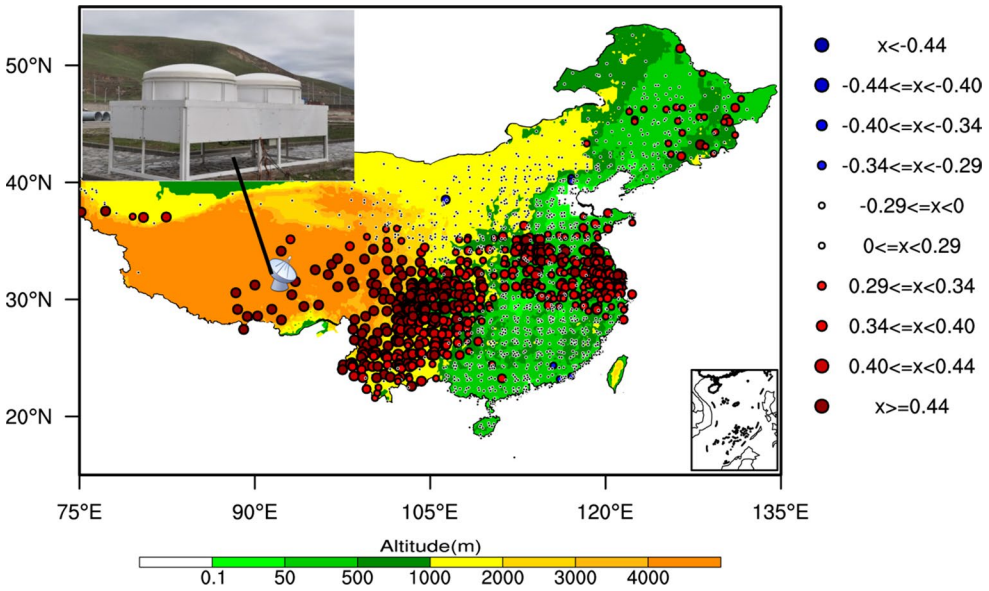

Fig. 1 Correlation coefficient between cloud cover detected by the observation station in Naqu in the summer and the total cloud cover detected countrywide via 1856 observation stations for the summers from 1961 to 2010. Note: Red and blue circles indicate positively and negatively correlated observation stations, respectively, with correlation coefficients of 90% or higher. The colors indicate the topographic altitudes of China (unit: m). Note: the radar mark indicates the specific location of the C-FMCW radar in Naqu. The small radar picture in Fig. 1 shows the location and actual image of the C-FMCW radar in Naqu during the Third Tibetan Plateau atmospheric experiment in 2014

the convective clouds over Naqu detected via radar echoes possess predictive strong-signal characteristics with respect to the rainstorm cloud systems over the lower reaches of Naqu.

2 Instruments, data, and research methodology

2.1 C-FMCW radar

The target C-FMCW radar, which has vertical directionality, is mainly used to detect radial velocity, echo intensity, the spectral width of velocity, and echo power. Its technical parameters are as follows: the range of vertical detection is from 20 m to 15 km, the vertical resolution is 30 m, the temporal resolution is 3 s, and the operating frequency is 5530 ± 3 MHz. Ruan et al. (2015) noted that the C-FMCW radars have far lower noise levels for echo signals than the Doppler radars and wind profile radars. Thus, the C-FMCW radar has remarkable advantages when describing the vertical structural characteristics of precipitating clouds.

2.2 Data

Here, the researchers mainly used reanalysis data from the European Center for Medium-Range Weather Forecasts (ECMWF) (0.25° × 0.25°) from August 2014 as well as conventional statistics for specific humidity, horizontal wind field, and vertical velocity. Other research data included countrywide diurnal precipitation data from 2513 ground-based observation stations, countrywide diurnal total cloud cover data from 1876 observation stations, and echo intensity data from the C-FMCW radar site in Naqu (31.48°N, 92.06°E); these data were compiled in August 2014 during the Third TP Atmospheric Experiment.

2.3 Research methodology

2.3.1 Calculation method for whole-layer water vapor flux

The whole-layer water vapor flux is calculated using the following formulas:

$$\mathrm{qu}(x,y,t) = \frac{1}{g}\int_{p_t}^{p_s} q(x,y,p,t)u(x,y,p,t)\mathrm{d}p \tag{1}$$

$$\mathrm{qv}(x,y,t) = \frac{1}{g}\int_{P_t}^{P_s} q(x,y,p,t)v(x,y,p,t)\mathrm{d}p, \tag{2}$$

where g is the gravitational acceleration, u is the zonal wind, v is the meridional wind, q is the specific humidity, P_s is the atmospheric pressure at the Earth's surface, P_t is the atmospheric pressure at the top of the atmosphere, qu is the zonal water vapor flux, and qv is the meridional water vapor flux.

2.3.2 Calculation method for the correlation vector

Here, the researchers extracted the sample data detected from August 15th to 23rd, 2014 (at regular intervals of 6 h) and analyzed the three-dimensional correlation structures by utilizing correlation vector calculations and applying analysis methods to assess water vapor transport. This method adopts the Naqu radar echo intensity extremum to reflect the structural changes in the strong-signal factor of convection over the center of the plateau. To determine the indicative significance of the radar echo intensity observed at Naqu for water vapor transport, this paper analyzes the correlation between radar echo intensity and water vapor transport. Calculating the correlation between the whole layer or a single-layer vapor flux field and radar echo intensity is based on Pearson linear cross-correlation. These formulas are listed as follows:

$$R_{\mathrm{u}} = 1/(n-1) \cdot \frac{\sum_{i=1}^{n} \left(x_{\mathrm{ki}} - \bar{x}_{\mathrm{k}}\right)\left(\mathrm{qu}_{\mathrm{li}} - \overline{qu}_{\mathrm{l}}\right)}{\left(x_{\mathrm{kstd}} \times \mathrm{qu}_{\mathrm{lstd}}\right)} \tag{3}$$

$$R_{\mathrm{v}} = 1/(n-1) \cdot \frac{\sum_{i=1}^{n} \left(x_{\mathrm{ki}} - \bar{x}_{\mathrm{k}}\right)\left(\mathrm{qv}_{\mathrm{li}} - \overline{\mathrm{qv}}_{\mathrm{l}}\right)}{\left(x_{\mathrm{kstd}} \times \mathrm{qv}_{\mathrm{lstd}}\right)}, \tag{4}$$

where x_{ki} is the radar echo intensity; $\bar{x}_k$ is the average radar echo intensity; n is the number of samples; qu_{l} and qv_{l} are the zonal and meridional water vapor fluxes of the whole layer or a single layer, respectively; and x_{kstd}, $\mathrm{qu}_{\mathrm{lstd}}$, and $\mathrm{qv}_{\mathrm{lstd}}$ are the standard deviations of the radar echo intensity and zonal and meridional water vapor fluxes, respectively.

The Pearson linear correlation coefficient r (R_{u} or R_{v}) can be tested against the null hypothesis using the statistic:

$$t = r \cdot \sqrt{(n-2)/(1-r^2)}. \tag{5}$$

This test has a Student t distribution with $n - 2$ degrees of freedom.

The mathematical model of vector correlation is:

$$\vec{R}(x, y) = \vec{i}R_{\mathrm{u}}(x, y) + \vec{j}R_{\mathrm{v}}(x, y), \tag{6}$$

where $\vec{R}$ is the composite correlation vector, $R_{\mathrm{u}}(x, y)$ is the correlation coefficient field between the echo intensity extremum sequence and the qu component of the zonal water vapor flux, and $R_{\mathrm{v}}(x, y)$ is the correlation coefficient field between the echo intensity extremum sequence and the qv component of the meridional water vapor flux (Xu et al. 2008; Zhao et al. 2016a).

3 Convection characteristics detected by the C-FMCW radar site in Naqu

This paper focuses on a rainstorm belt that moved eastward from the TP from August 15th to 19th, 2014 (Fig. 2). As shown in Fig. 2, the rainstorm occurred over the Yangtze River Basin and the regions to the south. During its initial stage, rainfall was generated over the central and eastern TP (as shown by the red circles in Fig. 2a, b) with a diurnal rainfall amount of less than 20 mm. Subsequently, the rain belt moved eastwards. On August 17th (as shown by the red circle in Fig. 2c), the main body of the rain belt moved eastward to the upper and middle Yangtze River regions to the east of the TP (the amount of precipitation was greater than 50 mm, thus reaching the rainstorm grade). On August 18th, the main body of the rain belt reached the southern region of the middle Yangtze River (as shown by the oval in Fig. 2d). In certain regions, the amounts of precipitation achieved heavy rainstorm levels (i.e., exceeding 100 mm). The east end of the rain belt moved eastward to the estuary of the Yangtze River (as shown in Fig. 2d). On August 19th, the rainstorm belt moved eastward to the southeastern regions of China, and the main body of the rainstorm belt was located in South China (as shown by the red circle in Fig. 2e). This paper attempts to elucidate whether the evolutionary behaviors of the eastward-moving rainstorm over the Yangtze River Basin that originated over the central TP were significantly correlated to the "strong-signal" convection system in the atmosphere over a key area of the TP.

Related studies have noted that a radar echo intensity of greater than 35 or 40 dBZ indicates a meso-scale convective rain belt (Schumacher and Johnson 2005; Wang et al. 2014). Wang et al. (2015) noted that the development of strong meso- and microscale turbulence and convection was correlated to the total surface radiation intensity of the TP. In addition, the strong heat source on the ground surface or the complex topography of the central TP gave rise to strong thermodynamic nonuniformity at the surface. Therefore, the large-scale vertical movement over the TP was significantly correlated to the apparent heat source Q1 of the atmosphere. The results of their study uncovered the driving processes of the heat source and the contributions of the turbulent energy present in the convective motion over the southeastern edge of the TP to the genesis and development of convective cloud clusters. This paper compares the temporal vertical sections of the maximum echo intensities (as shown in Fig. 3a) from the C-FMCW radar site at Naqu for 6-h intervals from August 10th to 20th, 2014, the related vertical velocities, and the apparent heat source Q1 obtained via ECMWF data calculations (as shown in Fig. 3b and c).

The results of a related study (Xu 2015) also showed that both the low cloud cover and the distribution of the

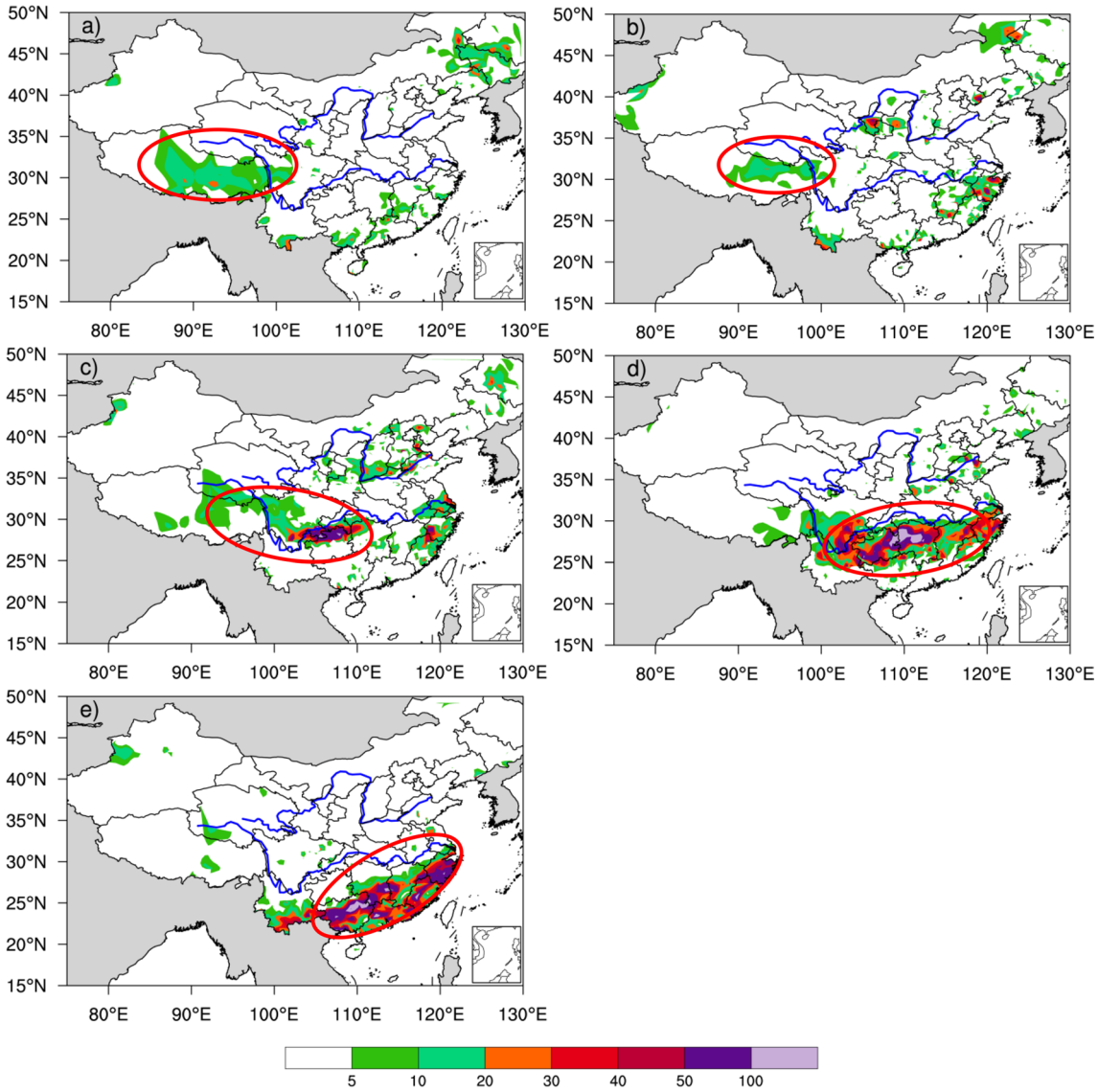

Fig. 2 Diurnal cumulative rainfall from August 15th to 19th, 2014 (unit: mm). Note: The colors in (**a**–**d**), and **e** indicate the diurnal rainfalls of August 15th, 16th, 17th, 18th, and 19th, respectively. Note: the northern and southern blue lines indicate the Yellow River and the Yangtze River, respectively

total cloud cover over the TP were significantly correlated to the whole-layer apparent heat source of the TP. Furthermore, these research results uncovered the main channels for the low- and mid-altitude water vapor transports driven by the heat source columns over the central and eastern TP regions with the frequent occurrences of convective clouds. The results showed that the abnormal cloud structure characteristics over the TP were closely correlated to the whole-layer heat source intensities. The current study also uncovered significant correlations between the apparent heat source Q1, vertical velocity, and convection characteristics indicated by the radar echoes in the Naqu region. According to the calculation results, the strong echo areas (indicated via the black circles in Fig. 3a) are significantly correlated to the vertical velocity and whole-layer apparent heat source Q1 (available in the reanalysis data) (see Fig. 3b, c) in terms of their vertical layers and times. Specifically, from August 10th to 11th, 14th to 16th, and 19th to 20th, the radar echo intensities could be divided into five high-value areas (indicated by black circles) from the ground surface to heights of 3 km. The high-value areas of the whole-layer apparent heat source Q1 and the vertical velocity (indicated by red circles) are available for the time ranges associated with these dates. In addition, the calculation results show that the strong echoes received by the C-FMCW radar in Naqu can

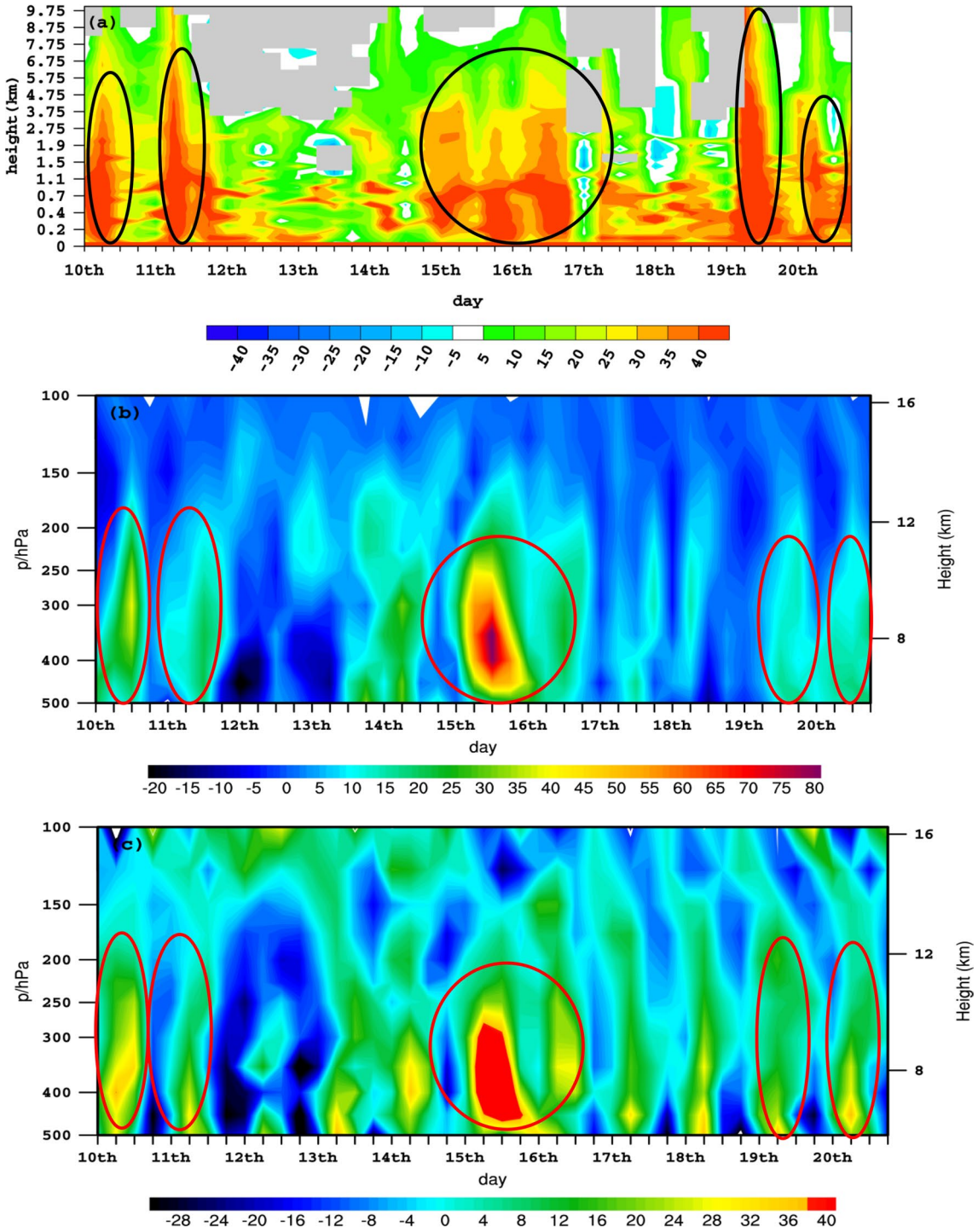

Fig. 3 **a** Time-varying vertical section of the maximum echo intensity of the C-FMCW radar site at Naqu at 6-h intervals from August 10th to 20th, 2014 (unit: dBZ). **b** Time-varying vertical sections of vertical velocities (unit: − 0.01 hPa/s); **c** time-varying vertical sections of the apparent heat source Q1 (unit: K s^{-1}) (note: area A is the source area of the three rivers and is highly correlated to the heat source); **d** correlation between the echo intensity of the C-FMCW radar and whole-layer heat source during the precipitation process (note: the correlation region A is the source area of the three rivers); **e** correlational relationship between the maximum echo intensities (unit: dBZ) measured at 6-h intervals at heights of 300–400 hPa from August 10th to 20th and the vertical velocities (hPa/s) at the same heights during the same period; **f** correlational relationship between the maximum echo intensity (unit: dBZ) and apparent heat source (K s^{-1}) for the same case as **e** (note: the black circle in **a** and the red circles in (**b**) and **c** indicate salient regions with strong echoes, strong upward movements, and strong thermodynamic effects; the correlation coefficients in (**e**) and **f** pass the 90% significance test)

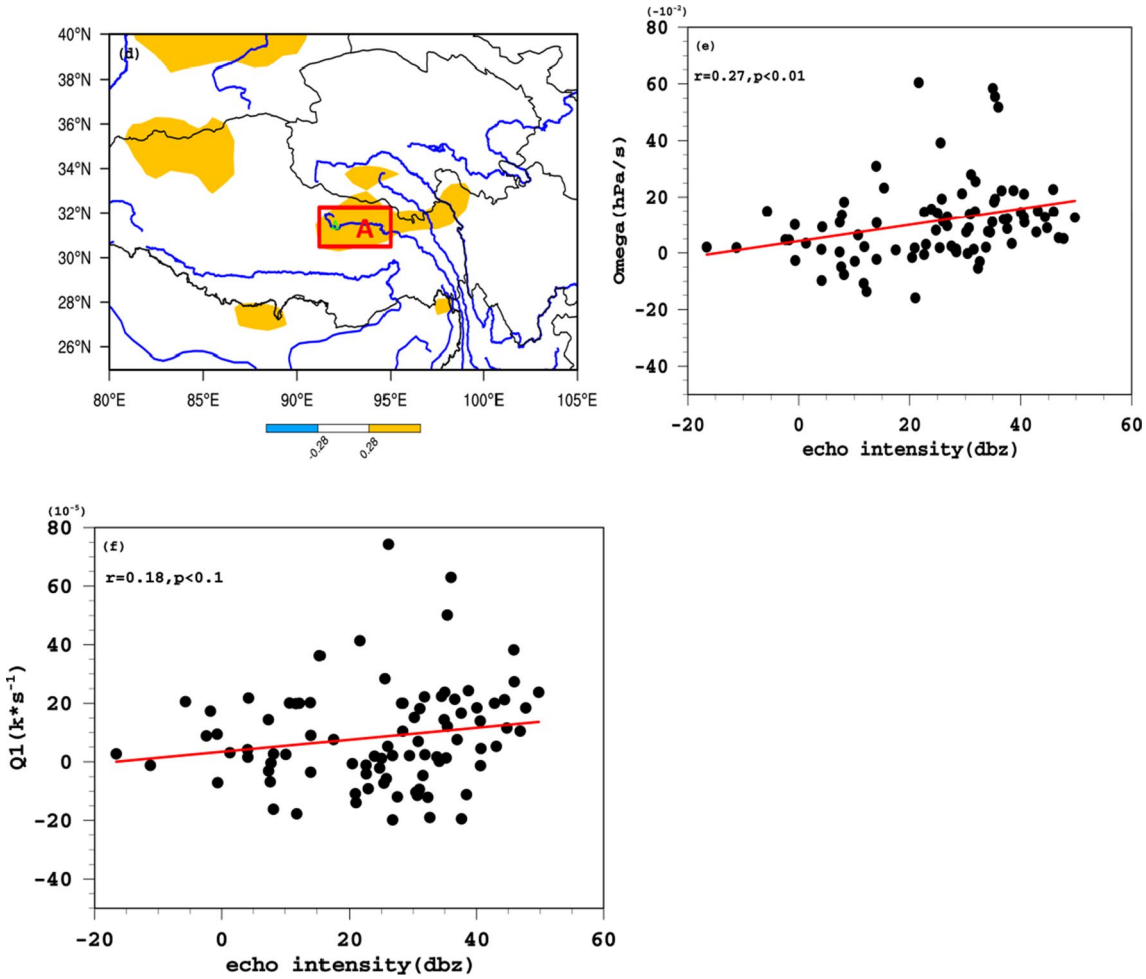

Fig. 3 (continued)

reflect both the convection status over the central TP and the regional heat source structures. As shown in Fig. 3d, the center of the extreme values of the high correlation between the echo intensity of the C-FMCW radar and the regional whole-layer apparent heat source Q1 values over the TP occurs over the well-known source area of the three rivers in the TP (i.e., the Yellow River, Yangtze River, and Lancang River). This paper analyzes the scatter diagram results of the extreme correlation values of the radar echo intensity and vertical velocity, as well as the whole-layer apparent heat source Q1 at 300 to 400 hPa from August 10th to 20th (Fig. 3e, f). The credibility of the correlation is calculated to be greater than 90% at 400–300 hPa. The above research results show that the echo intensity of the C-FMCW radar has remarkable indicative significance for the local whole-layer apparent heat source Q1 and the vertical velocities related to the development of convection. The atmospheric heat sources of the TP are known to exert a significant influence on the process of cloud precipitation and the water vapor transport flow patterns in local regions and the lower reaches of the Yangtze River. Based on analyses of the correlations between the echoes of the C-FMCW radar site at Naqu, which is located in the central TP and characterized by frequent convection activities, as well as the local convection characteristics and heat sources, this paper mainly discusses the relationship between the changes in C-FMCW radar echoes at Naqu and the evolutionary processes of eastward-moving rainstorm belts over the lower reaches of the TP. This paper also addresses the debate of how to connect the upstream precursory strong-signal characteristics of convective clouds with downstream rainstorms.

4 Correlation between the local convection characteristics of the TP and the three-dimensional structure of water vapor transport

During the summer, the heat sources of the TP constitute a powerful kinetic pump, which constantly attracts warm and moist air from low-latitude ocean regions (Wu and Zhang 1998), thus forming a cross-hemisphere atmospheric water circulation structure. The southern and eastern parts of the TP are associated with planetary-scale circulations that span the northern and southern hemispheres as well as the eastern and western hemispheres. Upon arriving at the TP, warm and moist oceanic air climbs the southern slopes of the TP, causing frequent convective activity (Xu et al. 2004).

This paper analyzes the three-dimensional atmospheric structures and water vapor transport characteristics of Naqu. As shown in Fig. 4a and b, the atmospheric structures associated with the triggering mechanisms of convective cloud systems are characterized by a feature wherein the layers at 100 and 200 hPa have the same divergence area as the water vapor flux. In the divergence area, the layer at 200 hPa is located within an anticyclonic circulation system (Fig. 4b), and the middle and low layers at 300 hPa (Fig. 4c) and 400 hPa (Fig. 4d) are located in the same convergence area (as indicated by the blue circles in Fig. 4c, d) of a southeasterly water vapor flow and a westerly water vapor flow, both of which have dipole structures comprising anticyclonic and cyclonic circulations. In addition, the correlation vector of the water vapor flux at 500 hPa has a strong convergence structure (Fig. 4e). According to the above research results, the coupling of the upper level divergence and lower level convergence related to the water vapor transport in the atmosphere and the dipole circulation structure in the middle layer of the atmosphere constitute important mechanisms for the stimulation and maintenance of convective clouds over the areas of the TP with frequent convective activities.

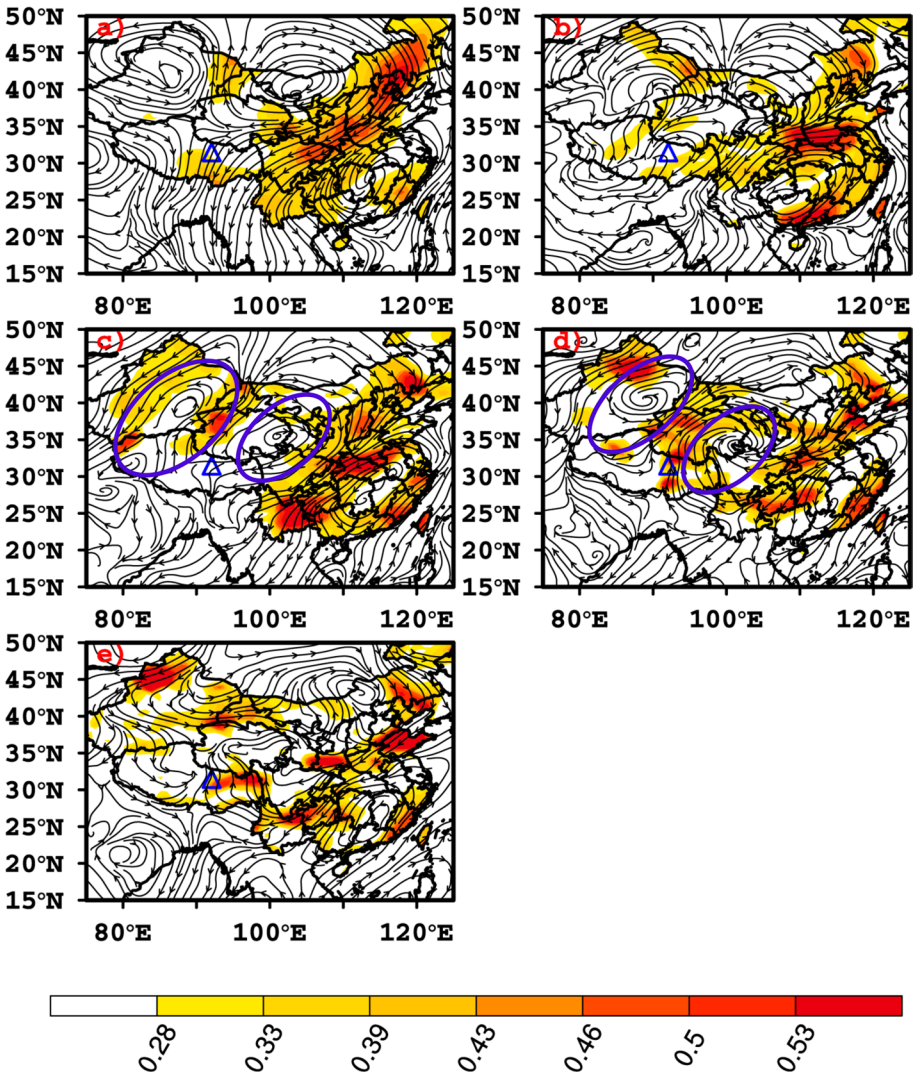

Fig. 4 Flow field of correlations between the maximum echo intensities (unit: dBZ) of the C-FMCW radar site at Naqu at 6-h intervals from August 15th to 23rd, 2014 and the water vapor transport fluxes (unit: g cm^{-1} s^{-1} hPa^{-1}) at the corresponding times (note: the heights in (**a**–**e**) are 100, 200, 300, 400, and 500 hPa, respectively). The colors indicate the maximum absolute values of the correlation coefficients of the water vapor flux components (qu or qv) with the maximum echo intensity, which are correlated at the 90% confidence level. The blue triangle indicates the location of the C-FMCW radar in Naqu, and the double ellipses in (**c**) and **d** indicate dipole-correlated circulations

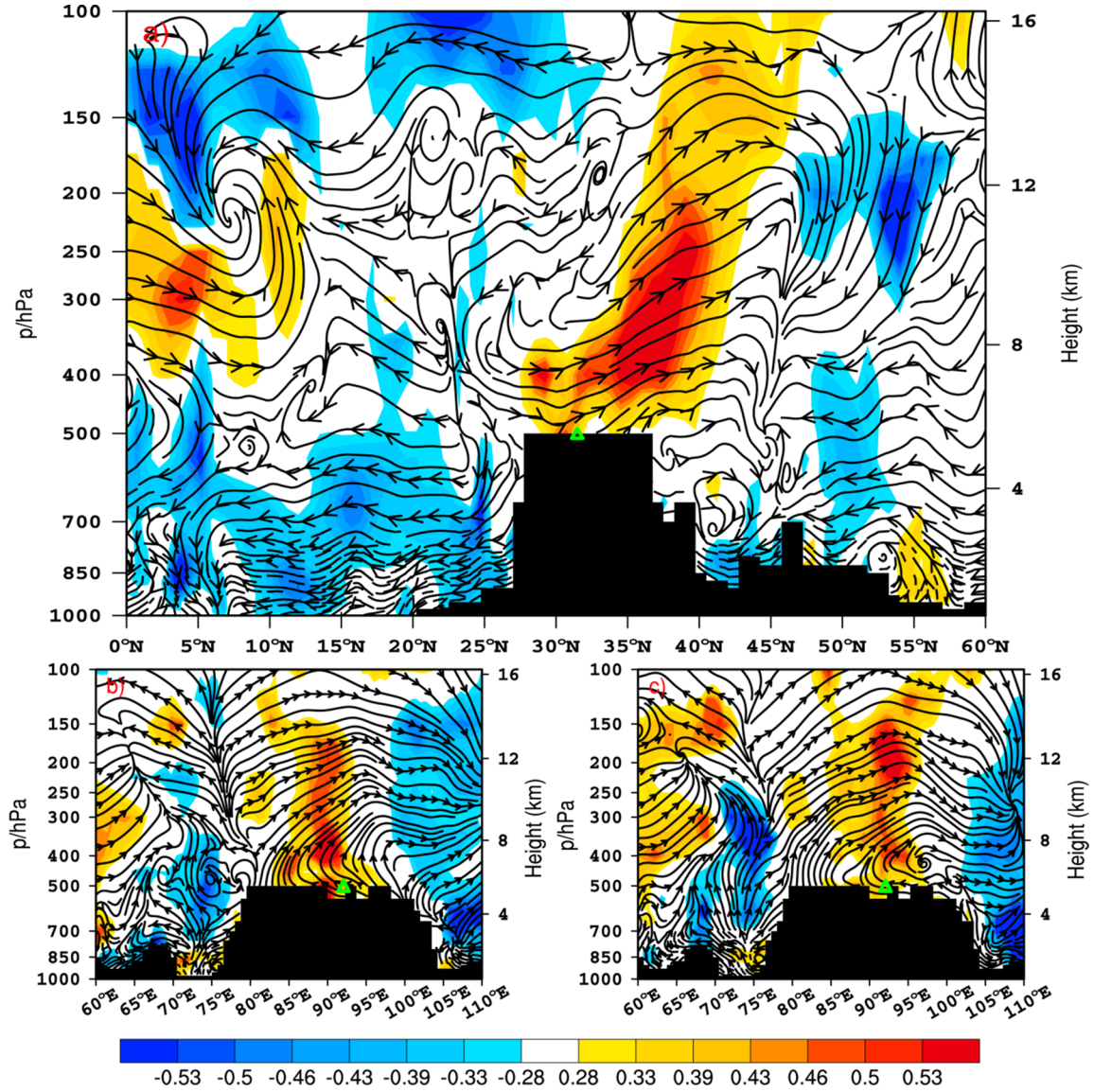

Fig. 5 **a** Section showing the meridional correlations of the maximum echo intensities of the C-FMCW radar site at Naqu at 6-h intervals from August 15th to 23rd, 2014 and the vw flow fields (92°E) at the same times; **b** section showing the zonal correlations of the maximum echo intensities (unit: dBZ) from August 15th to 23rd, 2014 and the uw flow field (12 h earlier) (31°N); **c** section showing the zonal simultaneous correlations of the above sections. Note: The colors indicate confidence levels greater than 90%; the green triangle indicates the specific location of the C-FMCW radar at Naqu

According to the vertical sections related to the correlations of the echo intensities of the C-FMCW radar site in Naqu and the south–north wind field (92°E) (shown in Fig. 5a), a southerly airflow is dominant over the southern TP, and the main body of this airflow is gradually transformed into a strong updraft (500–200 hPa) in the lower layer of the atmosphere over Naqu. The convection activities in Naqu are clearly significantly correlated to the low-layer southerly wind and the ascending branch of the local airflow. This conclusion is consistent with the strong convergence structure of the water vapor flows at 500 hPa over Naqu, as shown in Fig. 4. In addition, Fig. 5b, c shows the vertical sections related to the correlations between the echo intensities of the C-FMCW radar site at Naqu and the west–east wind field (31.5°N). In Fig. 5b, the wind field is presented 12 h early. Figure 5c shows the vertical section related to the simultaneous correlation between the echo intensities and the wind field. Comparing Fig. 5b, c reveals that the development process of the convection activities in Naqu is closely correlated to the westerly water vapor flows and ascending motion. The composite analysis of Fig. 5a–c reveals that the genesis and development of convective clouds in Naqu are correlated to the eastward-moving system, the local thermodynamic effects of the TP,

and the convergence of the westerly and southerly water vapor flows over the TP.

5 The strong-signal characteristics of upstream convective clouds over the TP during a rainstorm event in the Yangtze River Basin

In 1991 and 1998, the Yangtze River Basin experienced rare continuous rainstorm-induced flooding events with an initial cloud system that could be traced back to the central TP (Xu et al. 2002). The question remains: why are the frequent eastward-moving convective cloud systems in the TP and the water vapor transports of sensitive regions related to the rainstorm events over the upper reaches of the Yangtze River Basin?

In terms of the water vapor transport related to the summer precipitation over China, the TP, Indian Ocean, Bay of Bengal, and South China Sea are all involved in the transport of monsoon moisture into China; these regions are the key areas that give rise to the abnormal drought and flood conditions in China (Xu and Chen 2006; Xu et al. 2013). Related research has noted that the circulation features in the atmosphere over the TP favor the development of low-layer convection, indicating that the strong convections of the central and eastern TP are strongly correlated to the release of the latent heat of moisture (Zhu and Luo 1986; Wang et al. 2012; Zhu et al. 2012). Overall, multiple observational studies have shown that the rainstorm systems over the lower reaches of the TP can be traced back to the convective cloud systems in the atmosphere of the TP. Zhao et al. (2016b) noted that the turbulent structure of the water vapor flux of the atmosphere over the TP was significantly correlated to an eastward-moving precipitation system that progressed to the lower reaches of the TP. This paper probes the dynamic structures of those convection systems that are closely correlated to the rainstorms over the Yangtze River Basin as well as the characteristics of its water vapor transport channels. Figure 6 shows the correlation between the diurnal total cloud cover variations detected by the single observation station at Naqu and the diurnal total cloud cover variations detected throughout all of China via 1876 observation stations in August 2014. There exists an obvious belt-shaped correlation structure for the total cloud cover (indicated by the black frame) in the areas from the eastern TP to the lower reaches of the Yangtze River, demonstrating that the cloud system in Naqu is significantly correlated to the eastward movements of the cloud systems in the regions ranging as far as the lower reaches of the TP.

Figure 7 shows the vertical sections related to the correlations between the maximum echo intensity of the C-FMCW radar site at Naqu during August 15th to 23rd, 2014, and the water vapor states (i.e., specific humidity) at different heights along the latitude of 31.5°N at different lag times: (a) simultaneous and at time lags of (b) 24, (c) 48, and (d) 72 h (note: the colors reflect credibility). Overall, the correlations between these data sets at different lag times are reflected by the dynamic eastward-moving water vapor column. According to the research results, the water vapor column (i.e., the section along the latitude of 31.5°N) is indicative of a simultaneous correlation at a slightly western position (blue frame in Fig. 7a) in Naqu (green triangle). The vertical section of the water vapor column shows a high correlation with a time lag of 24 h moving eastward to the central and eastern TP (blue frame in Fig. 7b). The water vapor column further shows a high correlation with a time lag of 48 h moving eastward to the eastern border of the TP (Fig. 7c) and a high correlation with a time lag of 72 h beyond the TP, reaching the central and eastern regions of China (blue frame in Fig. 7d). In summary, the changes in the echo intensity of the C-FMCW radar site at Naqu possess predictive strong-signal

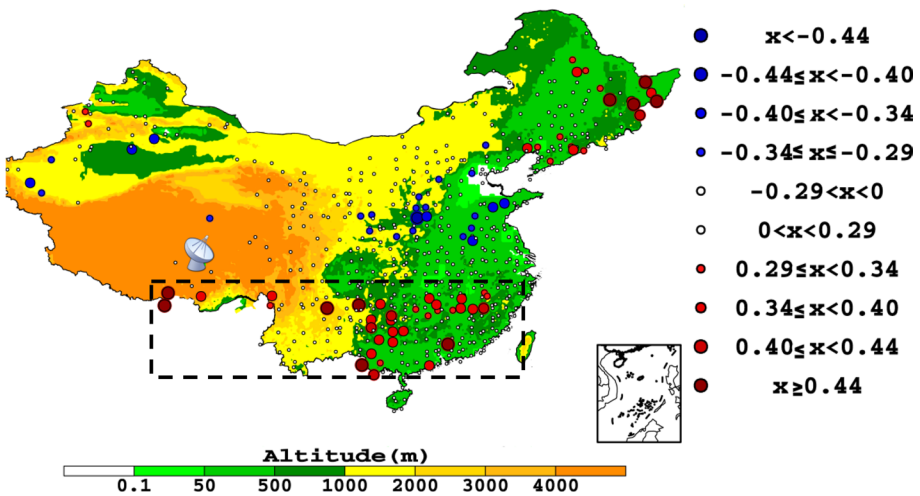

Fig. 6 Correlation between the diurnal total cloud cover variations detected by the single observation station at Naqu and the diurnal total cloud cover variations detected countrywide at 1876 observation stations in August 2014. Note: the radar mark indicates the specific location of the C-FMCW radar of Naqu

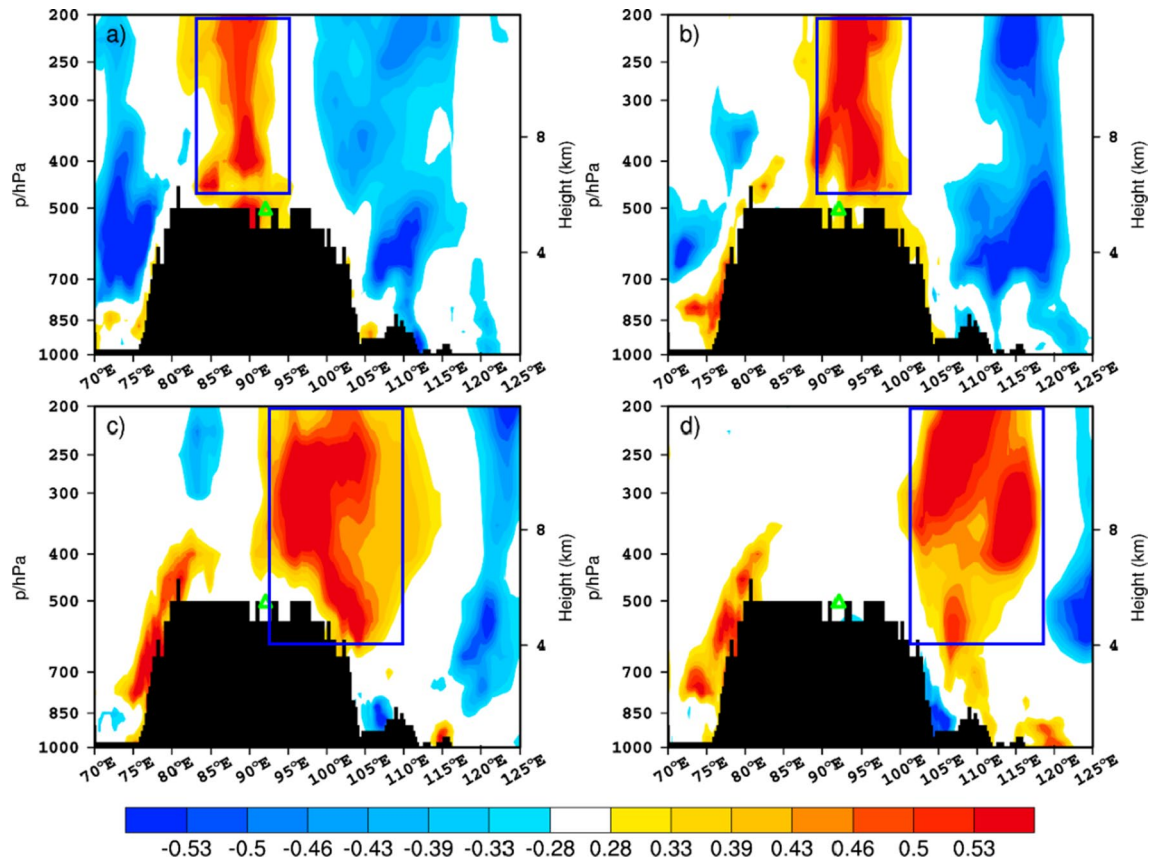

Fig. 7 Vertical section showing the correlation between the maximum echo intensity (unit: dBZ) of the C-FMCW radar site at Naqu from August 15th to 23rd, 2014, and the water vapor state (unit: kg/kg) at different heights along the latitude of 31.5°N at different lag times: **a** simultaneous, **b** a time lag of 24 h, **c** a time lag of 48 h, and **d** a time lag of 72 h. Note: the colors indicate that the confidence level is greater than 90%. The green triangle indicates the specific location of the C-FMCW radar in Naqu

characteristics with respect to the state of the water vapor column converging in the vicinity of the eastward-moving precipitation system over the lower reaches of Naqu. Therefore, these dynamic changes are of certain indicative significance for the genesis of extreme rainstorm events over the lower reaches of the TP.

This paper calculates the vector field of the correlation between the maximum echo intensity of the C-FMCW radar site at Naqu and the water vapor transport flux at 200 and 500 hPa from August 15th to 23rd, 2014 (Fig. 8). In addition, this paper shows the correlation between the changes in the echo intensity of the C-FMCW radar on the TP and the spatiotemporal evolution of the eastward-moving rainstorm system in the lower reaches of the TP. As shown in Fig. 8a, b, the vector field of the simultaneous correlations between the changes in the echo intensities of the C-FMCW radar site at Naqu and the water vapor transport fluxes at high and low atmospheric layers can reflect the coupling of the upper level divergence and low-level convergence at Naqu as well as the rain belt (indicated by the red circle). Figure 8c, d shows the correlations between these features at a 24-h time lag. At this time, the correlation structure of the coupling of the upper level divergence and lower level convergence was related to the water vapor transport that originated in the central TP and moved to the eastern TP with a weakened west–east rain belt (indicated by the red circle). The upper level atmosphere over the precipitation area was characterized by anticyclonic circulation. Figure 8e, f shows the correlations of the echo intensity and water vapor transport at a time lag of 48 h. At this time delay, the correlation structure of the coupling of the upper level divergence and lower level convergence related to the water vapor transport left the TP and reached the eastern fringe of the TP (at approximately 30°N, 104.5°E). The correlation structure of this coupling was more significant here. In particular, the upper level anticyclonic circulation system was very prominent, and at the lower level, the correlation vector of the southerly and northerly water vapor flows presented a strong convergence pattern over the eastern TP. This pattern was accompanied by a west–east rainstorm belt (indicated by the red circle) with an abrupt change in the precipitation intensity. Figure 8g, h shows the correlations of the echo intensity and water vapor flux at a time lag of 72 h. At this time delay, the

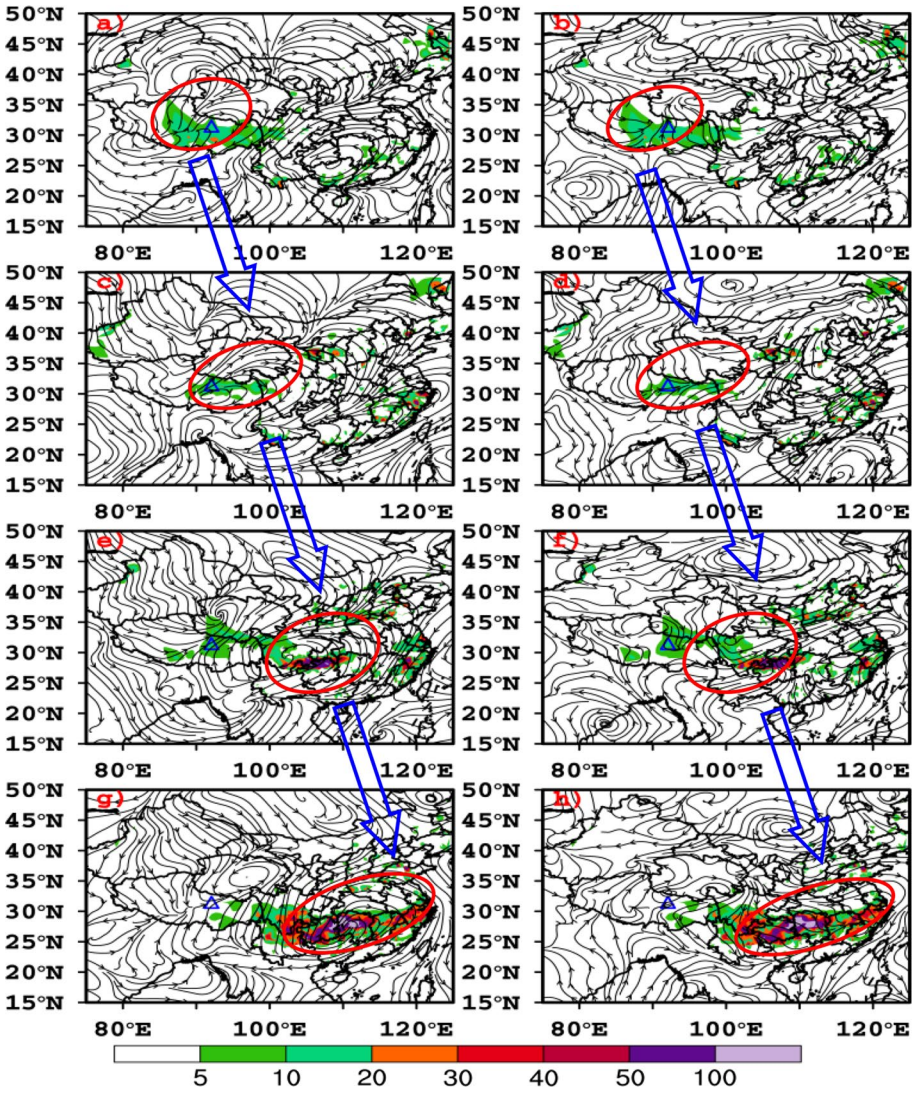

Fig. 8 Flow-field diagrams of the correlation between the maximum echo intensity (unit: dBZ) of the C-FMCW radar site at Naqu during August 15th to 23rd, 2014, and the single-layer water vapor transport flux (unit: g cm^{-1} s^{-1} hPa^{-1}) at 200 hPa and 500 hPa at different lag times: (1) simultaneous (**a**, **b**); (2) a time lag of 24 h (**c**, **d**); (3) a time lag of 48 h (**e**, **f**); and (4) a time lag of 72 h (**g**, **h**). Note: The colors indicate the diurnal amounts of precipitation from August 15th to 18th; the height is 200 hPa in (**a**, **c**, **e**, **g**) and 500 hPa in (**b**, **d**, **f**, **h**); the green triangle indicates the specific location of the C-FMCW radar in Naqu; the red circles indicate the key areas of precipitation; and the blue arrows indicate the movement directions of precipitation

correlation structure of the coupling of the upper level divergence and lower level convergence related to the water vapor transport moved to the middle and lower reaches of the Yangtze River. Within the west–east rainstorm belt, a large-scale anticyclonic circulation was detected that covered China's southern regions at the upper level, and a large-scale cyclonic circulation was detected in the middle and lower reaches of the Yangtze River in an axial direction at the lower level. The core area of the rainstorm belt was characterized by the correlation vector of a strong convergent water vapor flow.

6 Strong-signal characteristics of the apparent heat source in the central TP and the variety of rainstorm processes in the lower reaches of the TP

Due to the thermal effects of the TP and its unique topographic characteristics, the TP serves as a transfer point and transports monsoon water vapor to the Yangtze River Basin. During the years when the Yangtze River Basin

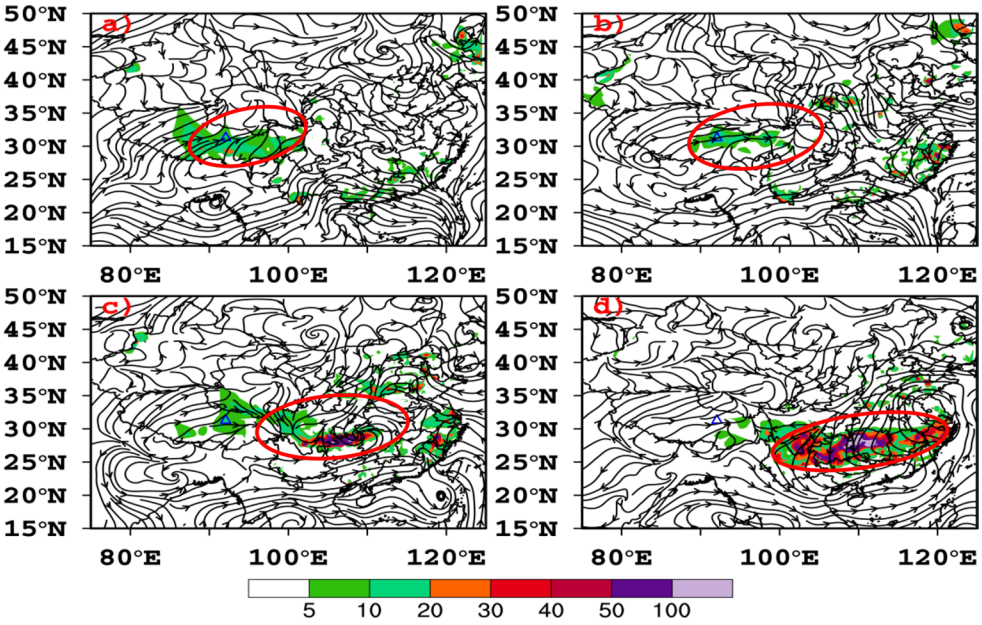

Fig. 9 Correlation between the whole-layer apparent heat source Q1 (unit: w/m^2) in the source area of three rivers and the whole-layer water vapor transport flux (unit: g s^{-1} hPa^{-1} cm^{-1}) at different lag times: **a** simultaneous; **b** a time lag of 24 h; **c** a time lag of 48 h, and **d** a time lag of 72 h. Note: The colors indicate the amounts of precipitation (unit: mm), and the red circles indicate the main precipitation occurrence areas

suffers droughts or floods, the water vapor distribution characteristics over the TP and monsoon regions are also abnormal.

Experimental research has indicated that the structural changes in the convection of the central plateau are indicated by strong-signal factors; thus, the changes in the echo intensity of the C-FMCW radar site at Naqu are of remarkable indicative significance for the whole-layer apparent heat source Q1 and the development of convection. The area with a high correlation between the changes in the echo intensity of the C-FMCW radar site at Naqu and the whole-layer apparent heat source Q1 was exactly adjacent to the well-known source area of the three rivers (as shown in area A in Fig. 3d). Figure 9 shows the characteristics of the correlations between the regional whole-layer apparent heat source Q1 in the well-known source area of the three rivers and the dynamic evolution of the eastward-moving rainstorm belt over the middle and lower reaches of the Yangtze River from August 15th to 23rd, 2014, at different lag times: (a) simultaneous and at time lags of (b) 24, (c) 48, and (d) 72 h. Note that the changes in the apparent heat source in the source area of the three rivers are correlated to the echo intensities of the C-FWCW radar site at Naqu and could provide both predictive strong-signal characteristics of the spatiotemporal evolution of the rainstorm system and reproductions of the three-dimensional structures of the correlation between the convective activities and thermodynamic effects of the TP and the spatiotemporal evolution of the eastward-moving rainstorm system over the Yangtze River Basin. This conclusion further demonstrates that with the topographical thermo-driving effects of the TP, the changes in the cloud structures in the central TP with frequent convective activities can provide strong predictive signals of the genesis and development of rainstorms over the Yangtze River Basin.

7 Conclusions and discussion

To analyze the rainstorm processes that occurred in the middle and lower reaches of the Yangtze River Basin during August 15th to 19th, 2014, this study extracted sample data from August 15th to 23rd, 2014 (at regular intervals of 6 h) as well as dynamic data of the echo intensities from the C-FMCW radar site at Naqu. Based on the dynamic statistics related to the three-dimensional correlation structures, this work aimed to capture and track the strong-signal characteristics indicated by the convection structures of the circulation systems in the key area of the TP during the genesis and development of the rainstorm.

By analyzing the three-dimensional atmospheric structure and the water vapor transport characteristics at Naqu (an area in the central TP with frequent convective activities), this paper found that the atmospheric structures involved in the triggering mechanisms of the convective cloud system had the following characteristics: (1) in the upper level of the correlation vector field, there existed an anticyclonic circulation with a divergence of water vapor flux; and (2) at the middle and low levels of the correlation vector field, there existed an area with strongly converging water vapor flows, specifically characterized as a dipole structure comprising anticyclonic and cyclonic circulations. Experimental research indicated that the coupling of the upper level divergence and lower level convergence with respect to the water vapor transport in the atmosphere to the dipole

circulation structure in the middle layer of the atmosphere constituted an important mechanism for the stimulation and maintenance of convective clouds in the TP with frequent convective activities.

Our analysis uncovered a correlation between the changes in the echo intensities of the C-FMCW radar of the TP and the spatiotemporal evolution of an eastward-moving rainstorm system over the lower reaches of the plateau. The intensity changes of the frequency-modulated echoes received by the C-FMCW radar located in Naqu possessed predictive strong-signal characteristics with respect to the status of the water vapor column converging near the eastward-moving precipitation system over the lower reaches of Naqu. Overall, the dynamic water vapor column moved eastwards. In the lag correlation diagram showing the water vapor transport flux, the coupling structure of the upper level divergence and lower level convergence was characterized by a trend of eastward movement and changed dynamically with the expansion of the rain belt. Strong convergence characteristics became increasingly obvious between the upper level large-scale anticyclonic circulation, the low-level cyclonic circulation, and the core area of the rainstorm belt.

According to our analysis, the changes in the echo intensity of the C-FMCW radar site at Naqu were of remarkable indicative significance to the whole-layer apparent heat source Q1 in local areas and in the adjacent well-known source area of the three rivers of the TP and the development of convection. The echo intensity of the C-FMCW radar could thus be used to indicate the regional heat source effect and the driving force behind local convection activities. Importantly, the changes in the apparent heat source of the three-river source area were correlated to the echo intensities of the C-FMCW radar site at Naqu and were also of predictive significance for the spatiotemporal evolution behaviors of the rainstorm system over the Yangtze River Basin and China's southern regions, including the lower reaches of the TP. Figure 10 shows the three-dimensional correlation structure of the precipitation system related to the eastward-moving rainstorm belt over the Yangtze River Basin. As shown in Fig. 10, a correlation structure exists between the anticyclonic divergence and the changes in the echo intensity of the C-FMCW radar site at Naqu, which was correlated to the apparent heat source of the central TP and the correlation vector field of the water vapor transport flux at 200 hPa and lag times of 24, 48, and 72 h. The correlation structure of the anticyclonic divergence at the upper atmospheric level increased with the development of the rainstorm belt. The correlation structures of the significant convergences of the middle and low atmospheric levels (at heights of 500 and 700 hPa) occur simultaneously and at lag times of 24 and 48 h. Finally, a correlation structure between the strong cyclonic convergence of the middle and low levels (at heights of 500 and 700 hPa) exists at a lag time of 72 h with the further development of the rainstorm belt. The above results show that with the topographic and thermal driving effects of the TP, the changes in the cloud structure in the central TP with frequent convective activities provide important predictive "strong signals" for the genesis and development of rainstorms over the Yangtze River Basin (shown in Fig. 10).

The present research is deficient in some respects. For example, the observation data acquired by the C-FMCW radar are very limited, and the continuity of the detection over space and time is not sufficient. In studying the

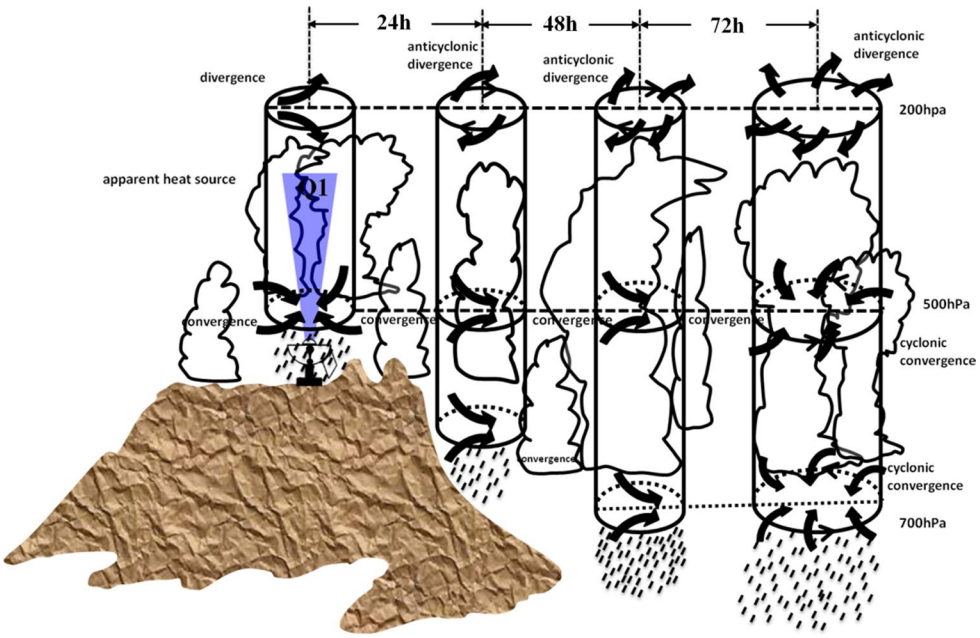

Fig. 10 Physical image of the comprehensive correlation between the strong-signal characteristics indicated by the echo intensity of the C-FMCW radar in the key area of convection in the TP and the process of the eastward-moving rainstorm belt in the middle and lower reaches of the Yangtze River

precursory strong-signal characteristics in an area ranging to the upper reaches of the rainstorm, the research selected only one individual case involving an eastward-moving rainstorm process from the observation data acquired by the C-FMCW radar sited in Naqu for nearly 40 days in 2014 during the Third TP Atmospheric Experiment. Further analysis is required to determine whether the genesis and development of heavy rainfall in the lower reaches of the TP are affected by other factors, such as differences in the intensity and spatiotemporal distribution of convective clouds, as well as differences in the structures of the cloud clusters moving away from the TP.

Acknowledgements The author is grateful for support of the following initiatives: (1) the Third TP Scientific Experiment, which is a Project supported by the Special Scientific Research Fund for Public Welfare Sectors (Meteorology) by the Ministry of Finance (GYHY201406001); (2) a major project supported by the National Natural Science Foundation of China (NSFC) (91644223); (3) a major project supported by the National Natural Science Foundation of China (NSFC) (91337000); (4) a consultative project supported by the Chinese Academy of Engineering (2017-XY-21); (5) the Jiangsu postgraduate research and innovation program project (1344051701002); and (6) the Jiangsu postgraduate research and innovation program project (KYCX17_0869).

References

Boos WR, Kuang Z (2010) Dominant control of the south Asian monsoon by orographic insulation versus plateau heating. Nature 463:218–222

Bringi VN, Keenan TD, Chandrasekar V (2001) Correcting C-band radar reflectivity and differential reflectivity data for rain attenuation: a self-consistent method with constraints. IEEE Trans Geosci Remote Sens 39:1906–1915

Cai WY, Xu XD, Sun JH (2012) Cloud status and surface energy budget in the southeastern Tibetan Plateau. Acta Meteorol Sin 70:837–846 **(In Chinese)**

Chang Y, Guo XL (2016) Characteristics of convective cloud and precipitation during summer time at Naqu over Tibetan Plateau. Chin Sci Bull 15(61):1706–1471 **(In Chinese)**

Flohn H (1968) Contributions to a meteorology of the Tibetan Highlands. Atmospheric Science Paper No. 130. Department of Atmospheric Science, Colorado State University, Fort Collins, Colo

Fu YF, Li HT, Zi Y (2007) Case study of precipitation cloud structure viewed by TRMM satellite in a valley of the Tibetan Plateau. Plateau Meteorol 26:98–106

Fujinami H, Yasunari T (2001) The seasonal and intraseasonal variability of diurnal cloud activity over the Tibetan Plateau. J Meteorol Soci Jpn 79:1207–1227

Hu L, Deng D, Gao S, Xu X (2016) The seasonal variation of Tibetan convective systems: satellite observation. J Geophys Res 121:5512–5525

Jin L, Ruan Z, Ge RS, Wu J, Qi R (2016) Application of FMCW technology in weather radar and cloud detection over the Tibetan Plateau. Mod Radar 38:6–11

Liu LP, Chu RZ, Song XM et al (1999) Summary and preliminary results of cloud and precipitation observation in Qinghai-Xizang Plateau in game-Tibet. Plateau Meteorol 18:441–450

Liu LP, Zheng JF, Ruan Z (2015) Comprehensive observation experiment on clouds and precipitations by diverse radars and preliminary analysis results of cloud characteristics in the Tibetan Plateau in 2014. Acta Meteorol Sin 10:635–647 **(in Chinese)**

Qin H (1983) Vertical distribution of atmospheric static energy during strong convective weather in Naqu, Tibetan Plateau. Plateau Meteorol 20:63–67 **(in Chinese)**

Ruan Z, Jin L, Ge R, Li F, Wu J (2015) C - Band FM continuous wave weather radar detection system and observation experiment. Acta Meteorol Sin 73:577–592

Schumacher RS, Johnson RH (2005) Organization and environmental properties of extreme-rain-producing mesoscale convective systems. Mon Weather Rev 133:961–976

Uyeda H, Yamada H, Horikomi J, Shirooka R, Shimizu S, Liping L, Ueno K, Fujii H, Koike T (2001) Characteristics of convective clouds observed by a Doppler radar at Naqu on Tibetan Plateau during the GAME-Tibet IOP. J Meteorolo Soc Jpn 79:463–474

Wang MR, Zhou SW, Duan AM (2012) Trend in the atmospheric heat source over the central and eastern Tibetan Plateau during recent decades: comparison of observations and reanalysis data. Chin Sci Bull 57:548–557

Wang H, Luo Y, Jou BJD (2014) Initiation, maintenance, and properties of convection in an extreme rainfall event during SCMREX: observational analysis. J Geophys Res 119:13206–213232

Wang YJ, Xu XD, Zhao TL, Sun JH, Yao WQ, Zhou MY (2015) Structures of convection and turbulent kinetic energy in boundary layer over the southeastern edge of the Tibetan Plateau. Sci China Earth Sci 58:1198–1209

Wu GX, Zhang YS (1998) Tibetan Plateau forcing and the timing of the monsoon onset over south Asia and the South China Sea. Mon Weather Rev 126:913–927

Xu XD (2015) Discussion of the effect and dynamic mechanism of the Tibetan Plateau. China Meteorological Press, Beijing, pp 17–18 **(in Chinese)**

Xu XD, Chen LS (2006) Advances of the study on Tibetan Plateau experiment of atmospheric sciences. J Appl Meteorol Sci 17:756–772

Xu XD, Tao SY, Wang JZ, Chen LS, Li Z, Wang XR (2002) The relationship between water vapor transport features of Tibetan Plateau-monsoon "large triangle" affecting region and drought-flood abnormality of China. Acta Meteorol Sin 60:257–266

Xu XD, Chen LS, Wang XR, Miao QJ, Tao SY (2004) Moisture transport source/sink structure of the Meiyu rain belt along the Yangtze River valley. Chin Sci Bull 49:181–188

Xu XD, Shi XY, Wang YQ, Peng SQ, Shi XH (2008) Data analysis and numerical simulation of moisture source and transport associated with summer precipitation in the Yangtze River Valley over China. Meteorol Atmos Phys 100:217–231

Xu XD, Lu CG, Ding YH, Shi XH, Guo YD, Zhu WH (2013) What is the relationship between China summer precipitation and the change of apparent heat source over the Tibetan Plateau? Atmos Sci Lett 14:227–234

Yanai M, Li CF, Song ZS (1992) Seasonal heating of the Tibetan Plateau and its effects on the evolution of the Asian summer monsoon. J Meteorolo Soc Jpn 70:319–351

Zhao Y, Xu XD, Chen B, Wang Y (2016a) The upstream "strong signals" of the water vapor transport over the Tibetan Plateau during a heavy rainfall event in the Yangtze River Basin. Adv Atmos Sci 33:1343–1350

Zhao Y, Xu XD, Zhao TL, Xu HX, Mao F, Sun H, Wang YH (2016b) Extreme precipitation events in East China and associated moisture transport pathways. Sci China Earth Sci 59:1854–1872

Zhu BZ, Luo MX (1986) Dynamic effect of orography on summer lower tropospheric circulation surrounding the Qingzang Plateau. Chin Sci Bull 31:827–830

Zhu XY, Liu YM, Wu GX (2012) An assessment of summer sensible heat flux on the Tibetan Plateau from eight data sets. Sci China Earth Sci 55:779–786

Zhuang W, Liu L (2012) A reflectivity climatology algorithm for hybrid scans and its application to radar coverage over the Tibetan Plateau. Acta Meteorol Sin 26:746–757

Zhuo G, Xu XD, Chen LS (2002) Instability of eastward movement and development of convective cloud clusters over Tibetan Plateau. Chin J Appl Meteorol 13:448–456